

This article was downloaded by:

On: 25 January 2011

Access details: *Access Details: Free Access*

Publisher *Taylor & Francis*

Informa Ltd Registered in England and Wales Registered Number: 1072954 Registered office: Mortimer House, 37-41 Mortimer Street, London W1T 3JH, UK



## Separation Science and Technology

Publication details, including instructions for authors and subscription information:

<http://www.informaworld.com/smpp/title~content=t713708471>

### Permeation of Gas Mixtures in Cellulose Acetate Membranes Practical Approach to Predict the Permeation Rate $\text{CO}_2/\text{CH}_4$ Mixture

A. E. Fouda<sup>a</sup>; T. Matsuura<sup>a</sup>; A. Lui<sup>b</sup>

<sup>a</sup> Division of Chemistry, National Research Council of Canada, Ottawa, Canada <sup>b</sup> Department of Chemical Engineering, University of Ottawa, Ottawa, Canada

**To cite this Article** Fouda, A. E. , Matsuura, T. and Lui, A.(1988) 'Permeation of Gas Mixtures in Cellulose Acetate Membranes Practical Approach to Predict the Permeation Rate  $\text{CO}_2/\text{CH}_4$  Mixture', *Separation Science and Technology*, 23: 12, 2175 – 2190

**To link to this Article:** DOI: 10.1080/01496398808075690

URL: <http://dx.doi.org/10.1080/01496398808075690>

## PLEASE SCROLL DOWN FOR ARTICLE

Full terms and conditions of use: <http://www.informaworld.com/terms-and-conditions-of-access.pdf>

This article may be used for research, teaching and private study purposes. Any substantial or systematic reproduction, re-distribution, re-selling, loan or sub-licensing, systematic supply or distribution in any form to anyone is expressly forbidden.

The publisher does not give any warranty express or implied or make any representation that the contents will be complete or accurate or up to date. The accuracy of any instructions, formulae and drug doses should be independently verified with primary sources. The publisher shall not be liable for any loss, actions, claims, proceedings, demand or costs or damages whatsoever or howsoever caused arising directly or indirectly in connection with or arising out of the use of this material.

PERMEATION OF GAS MIXTURES IN CELLULOSE ACETATE MEMBRANES  
- PRACTICAL APPROACH TO PREDICT THE PERMEATION RATE  
CO<sub>2</sub>/CH<sub>4</sub> MIXTURE<sup>a</sup>

A.E. Fouada, T. Matsuura  
Division of Chemistry  
National Research Council  
of Canada  
Ottawa, K1A 0R6, Canada

A. Lui  
Department of Chemical  
Engineering  
University of Ottawa  
Ottawa, K1N 6N5, Canada

ABSTRACT

Dry cellulose acetate reverse osmosis membranes of different porosities are prepared by using the solvent exchange method and then shrunk at various temperatures.

Permeation of single gases and gas mixtures of CO<sub>2</sub> and CH<sub>4</sub> through these membranes were investigated at various upstream pressures up to 2.4 MPa. The permeation data of a reference gas usually helium was used to characterize the membrane and determine the flow parameters which can be used to predict the performance of that membrane in separating gas mixtures. The Surface Force - Pore Flow model developed in previous investigations can be used to predict the membrane performance using the above method.

The prediction using the characterization parameters of the reference gas proved to be unsatisfactory in most cases, since the surface force is highly dependent on the interaction between the specific gas component in the mixture and the membrane.

---

<sup>a</sup> NRCC 28984

An alternative approach was used in this investigation, in which the permeation data of the gas mixture components were used to determine the flow model parameters and hence eliminate the gas-membrane interaction effects and produce better predictions for both the separation factor and flux. The results are shown for cellulose acetate membranes with a wide range of porosities which were dried using several combinations of solvents.

### INTRODUCTION

Cellulose acetate reverse osmosis membranes are generally prepared in a water-wet condition, and various techniques have been tested for the removal of the water to dryness. Solvent exchange techniques (1-6) can be used to dry the membranes and at the same time to preserve the membrane structure that is critical to the separatory performance and practical use in the gas separation application. Since permeation of single gases or gas mixtures through these membranes depends on the history of preparation, it is important to characterize each membrane, using permeation data for single gases at various pressures. This paper deals with characterization of membranes based on a gas flow mechanism through capillary "pores" (7). The concept of the "pore" used in this work is defined as "any space between nonbonded material entities in the membrane matrix, through which mass transfer can take place". The equivalent diameter of such a pore is expressed by some distance (however small) greater than zero (8).

The permeation data of gases through porous membranes were analysed based on the contribution of (1) Knudsen flow, (2) slip flow, (3) viscous flow, and (4) surface transport. The first three contributions are dependent mainly on the pore size as well as some physical parameters for the permeated gases. So, it was essential to assume a pore size distribution, for example, the normal or log-normal distribution.

This paper shows how to express these contributions mathematically using the log-normal pore size distribution and how to predict the performance of the membrane for the permeation of gas mixtures using the permeation data of pure gases in the same membrane.

There are, of course, other transport models which cannot be overlooked. Solution-diffusion model (9) and dual-mode sorption model (10) are far the most popular. However, there has been no attempt so far to predict the membrane performance data for the permeation of the gas mixture using the permeation data of

individual pure gases either by solution-diffusion or by dual-mode sorption model, particularly when membranes involved are of asymmetric structure. We have obtained satisfactory agreement between experimental permeation data and those calculated by using our model, and the prediction method is briefly outlined.

### THEORETICAL

The basic assumption in the Surface Force - Pore Flow model is that the effective membrane surface layer of an asymmetric porous cellulose acetate membrane is composed of a bundle of capillary tubes. Only the pores in the skin layer are considered to be active in the separation process. It is assumed that the pores are cylindrical and at right angles to the skin layer which has constant thickness. The transport through the membranes can then be expressed with appropriate transport equations for an individual cylindrical pore having an average radius and an average effective pore length and summed over all the pores in the membrane area; hence it is required to know the distribution of pore size. Although the normal distribution is often used to represent pore size, it has the disadvantage of allowing negative values, and negative pore dimensions are clearly impossible. To overcome this difficulty, the log-normal distribution law was adopted in the present work, and the pore size distribution can be represented by the following equation.

$$N(R) = \frac{N_t}{\sqrt{2\pi \ln \sigma_g}} \exp \left[ -\frac{1}{2} \left( \frac{\ln R - \ln \bar{R}}{\ln \sigma_g} \right)^2 \right] \quad (1)$$

For a single pore, the flow of gas can be described by one of the three mechanisms, namely (1) Knudsen flow; (2) slip flow; (3) viscous flow. The choice of a specific type depends primarily on the relative magnitude of the pore radius and the gas mean free path  $\lambda$ . Liepmann (9) limited the Knudsen flow to sizes where  $\frac{R}{\lambda} < 0.05$ . Stahl (10), on the other hand, suggested a slip flow mechanism in the range of  $\frac{R}{\lambda} = 1.5$  to 50, while viscous flow occurs for larger sizes ( $\frac{R}{\lambda} > 50$ ). So with a wide pore size distribution, one can expect the three mechanisms to occur simultaneously, but to different extents, depending on the operating conditions of pressure and temperature and the gas under study. The total quantity of gas permeation can be estimated by considering each pore and applying the relevant flow equation for gas transfer through it, then integrating the flow over the entire surface area.

For a single capillary, Present (11) derived the equations for Knudsen, slip, and viscous flows respectively as

$$q_k = \left( \frac{32\pi}{9MRT} \right)^{\frac{1}{2}} \frac{R^3 \Delta P}{\delta}, \quad q_{sl} = \frac{\pi R^3 \Delta P}{M\bar{c}\delta}, \quad \text{and} \quad q_v = \frac{\pi R^4 P \Delta P}{8\eta R T \delta} \quad (2)$$

where  $\bar{c}$  is the mean speed of gas molecules and is given by Metz (12) as:  $\bar{c} = (8\pi RT/\pi M)^{1/2}$

The total pore flow of the gas  $Q_g$  can be obtained by summing  $q_k$ ,  $q_{sl}$  and  $q_v$  over the pore size ranges applicable for each mechanism of transport as follows:

$$Q_g = \sum_{R=R_{\min}}^{R=0.05\lambda} N(R) q_k + \sum_{R=0.05}^{R=50\lambda} N(R) q_{sl} + \sum_{R=50\lambda}^{R=R_{\max}} N(R) q_v \quad (3)$$

where  $N(R)$ , and ( $q_k$ ,  $q_{sl}$ , and  $q_v$ ) are represented by equations (1) and (2). The summation in equation (3) can be replaced by integration to give the following expression for the total pore flow of the gas:

$$Q_g = \frac{N_t \Delta P}{\delta} [G_1 I_1 + G_2 I_2 + G_3 I_3] \quad (4)$$

where:

$$G_1 = (32\pi/9M\bar{c})^{1/2}; G_2 = (\pi/M\bar{c}); G_3 = (\pi\bar{P}/8\eta RT) \quad (5)$$

and the integrals  $I_1$ ,  $I_2$  and  $I_3$  are numerical values of integrals dependent on the porous structure and defined in detail in reference (16).

In the similar way, it can be shown (7) that the transport of gas molecules under the influence of gas polymer interaction can be represented by the equation:

$$Q_s = A_2' \frac{I_4}{I_5} \bar{P} \Delta P \quad (6)$$

where  $I_4$  and  $I_5$  are also numerical values of integrals dependent on the porous structure and defined in reference (16). By defining the gas permeability coefficient,  $A_G$ , as the amount of gas permeating per second per unit area per unit pressure difference, and by denoting the membrane area as  $S$ , we get

$$A_G = \frac{Q_t}{S \cdot \Delta P} = \left( \frac{N_t}{S \cdot \delta} \right) (G_1 I_1 + G_2 I_2 + G_3 I_3) + \frac{A_2'}{S} \frac{I_4}{I_5} \bar{P} \quad (7)$$

$$A_G = A_1 (G_1 I_1 + G_2 I_2 + G_3 I_3) + A_2 \frac{I_4}{I_5} \bar{P} \quad (8)$$

Equation (8) represents the relationship between the permeability coefficient  $A_G$  and the average pressure  $\bar{P}$  across the membrane. It has four parameters which can be evaluated from the permeation data under different operating pressures;  $A_1$  is the parameter related to the pore structure,  $A_2$  is the parameter related to the surface transport and  $\bar{P}$  and  $Q_t$  which enable the calculation of the integrals  $I_1$ ,  $I_2$ ,  $I_3$ ,  $I_4$  and  $I_5$ .

PREDICTION OF  $\text{CO}_2/\text{CH}_4$  GAS PERMEATION RATE

Mazid et al. (16) reported in detail the method for calculating the total permeation rate for the gas mixture from the individual fluxes of the components as follows:

$$[\text{PR}] = J_1 + J_2 \quad (9)$$

The individual fluxes of the mixture components can be written as:

$$J_1 = (A_G)_1 (P_2 X_{\tilde{z}2} - P_3 X_{\tilde{z}3}) \quad (10)$$

where  $X_{\tilde{z}3}$  ( $i=1,2$ ) represents the mole fraction of gases 1 and 2 in the permeate and can be defined as follows:

$$X_{\tilde{z}3} = \frac{J_1}{J_1 + J_2} \quad \text{or} \quad X_{\tilde{z}3} (J_1 + J_2) - J_1 = 0 \quad (11)$$

$$X_{\tilde{z}3} + X_{\tilde{z}2} = 1 \quad (12)$$

According to Mazid et al. (13), the prediction of  $[\text{PR}]$  can be done as follows:

- (1) The given membrane is first characterized in terms of  $(A_1)_{\text{He}}$ ,  $(A_2)_{\text{He}}$ ,  $\bar{R}_{\text{He}}$  and  $(\sigma_g)_{\text{He}}$  by regression analysis of the permeation data.
- (2) From  $(A_2)_{\text{He}}$ , values for  $(A_2)_1$  and  $(A_2)_2$  are calculated using the following equation

$$(A_2)_1 = (A_2)_{\text{He}} \phi_1 \quad (13)$$

where  $\phi_1$  is called the relative surface transport coefficient.

- (3) From  $\bar{R}_{\text{He}}$ , values for  $\bar{R}_1$  and  $\bar{R}_2$  are calculated from the equation:

$$\bar{R}_1 = \bar{R}_{\text{He}} + \Delta_1 \quad (14)$$

where the quantity  $\Delta_1$ , is called the radius correction factor and can be obtained from the pure gases permeation data.

- (4) Calculate all quantities  $(G_1)_1$ ,  $(G_2)_1$ ,  $(G_3)_1$  using gas properties, and evaluate the integrals  $(I_1)_1$  through  $(I_5)_1$  using the values of  $\bar{R}_1$  and  $(\sigma_g)_{\text{He}}$  (16).

- (5) Solve the cubic equation (11) to calculate  $\tilde{x}_{13}$  and substitute its value into equation (12) to calculate  $\tilde{x}_{23}$ .
- (6) Calculate the individual fluxes of the mixture components from equation (10) and substitute into equation (9) to calculate [PR].

### EXPERIMENTAL

Figure 1 is the schematic diagram of the procedure to prepare the dry asymmetric cellulose acetate membranes. The membranes were cast at 65% relative humidity using a solution with the following composition (wt %): Cellulose acetate (Eastman 398-3), 17%; acetone, 69.2%; magnesium perchlorate, 1.45%; and water, 12.35%. The temperature of the casting solution was kept at 10°C, while the temperature of the surrounding atmosphere was kept at 30°C. The solvent evaporation time was 60 seconds and then the membrane was transferred to the gelation bath for 1 hour. To obtain different porosities, the membranes were divided into 5 groups and each group was shrunk for 10 minutes at one of the following temperature values: 70, 75, 80, 85 and 90°C.

The membranes were then dried using the solvent exchange drying method (6). In this method the water in the membranes was first replaced by a water miscible solvent which included either methanol and ethanol. In this way we avoid the simple evaporation of water from membrane, since this would cause the pore structure to collapse due to the action of interfacial tension created by the retreating water.

The first solvent was then replaced by a second solvent which included one of the following: carbon disulfide, isopropyl ether, triethyl amine and hexane. The membranes were then air dried and identified according to shrinkage temperature, first solvent, and second solvent respectively.

The membranes were then mounted in the testing cells and flushed with the feed gas. The pressure was varied in the range of 400 to 2400 kPa, and the permeate flow rate was measured at each pressure by a soap bubble meter. The permeation data for the reference gas (helium) as well as  $\text{CO}_2$  and  $\text{CH}_4$  gases were collected to characterize the membrane, and then the gas separation experiments for the system of  $\text{CO}_2/\text{CH}_4$  were conducted. The air in reverse osmosis cells and in the feed gas line was removed by flushing them with the feed gas mixture of carbon dioxide and methane. The mole fraction of  $\text{CO}_2$  in the feed was changed from 0.10 to 0.90. All the experiments were conducted at room temperature and the feed pressure was varied in the range of 400 to 2400 kPa abs. The permeate flow rate was also measured by a soap bubble meter. The composition of the gas permeate was

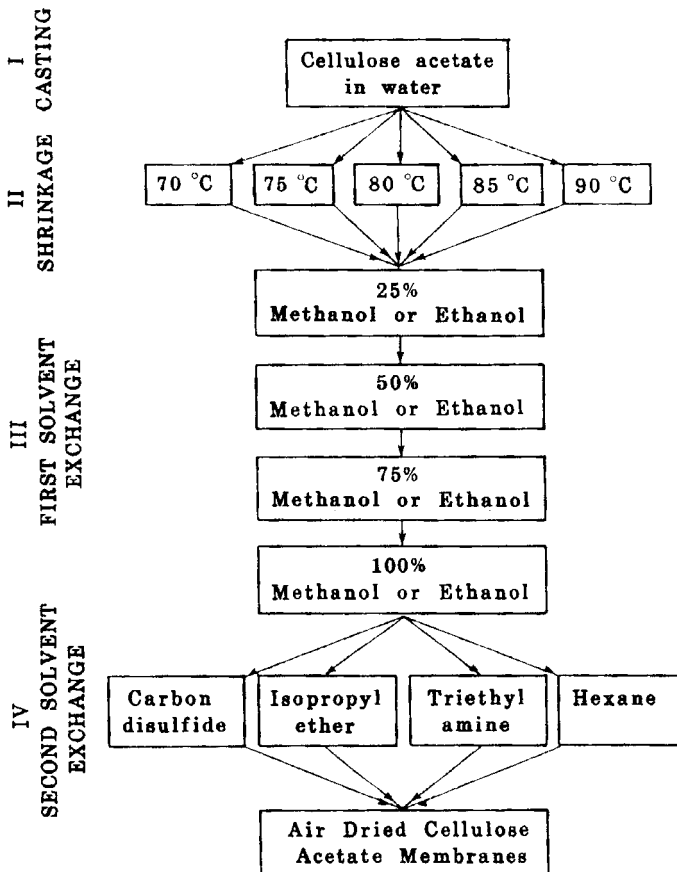


FIGURE 1 Schematic diagram for the preparation of dry cellulose acetate membranes by solvent exchange.

measured by gas chromatography using Tracor MT160/220 model equipped with a Porapak Q column.

#### RESULTS AND DISCUSSION

##### Characterization Parameters for Pure Gases

The permeation data were collected for helium, carbon dioxide and methane gases as volume flow rates at different pressure

Table 1 Membrane characterization by using helium permeation data

<sup>a</sup> Membrane	$(\bar{R})_{He} \times 10^{10},$ m	$(\sigma_g)_{He} \times 10^0,$ m	$(A_1)_{He} \times 10^{-20}$ m <sup>-3</sup>	$(A_2)_{He} \times 10^8$ kmol/m s Pa <sup>2</sup>
CA70-M-IPE	4.00	1.50	0.897	2.111
CA75-M-IPE	5.75	1.10	0.858	2.562
CA90-M-IPE	7.25	1.10	0.026	0.583
CA70-E-IPE	5.50	1.40	1.977	7.341
CA85-E-IPE	5.75	1.30	0.388	2.262
CA70-M-TEA	2.50	1.60	1.148	1.863
CA80-M-TEA	6.25	1.30	0.357	2.741
CA90-M-TEA	10.25	1.10	0.441	4.643
CA70-E-TEA	6.25	1.30	1.155	3.993
CA85-E-TEA	6.50	1.30	1.717	11.588
CA90-E-TEA	4.50	1.40	2.165	4.851
CA70-M-HEX	10.75	1.01	0.151	1.762
CA80-M-HEX	4.50	1.60	0.369	1.458
CA90-M-HEX	1.00	2.30	12.241	6.120
CA80-E-HEX	6.25	1.40	0.072	0.655
CA70-E-CS <sub>2</sub>	6.75	1.30	1.155	3.993
CA85-E-CS <sub>2</sub>	6.50	1.20	1.717	11.588
CA90-E-CS <sub>2</sub>	5.25	1.10	2.165	4.851

<sup>a</sup> This column indicates the membrane identification as follows:

1. The first part indicates the material and shrinkage temperature, e.g. CA75 means cellulose acetate membrane shrunk at 75°C.
2. The second part is the abbreviation for the first solvent which is M for methyl alcohol and E for ethyl alcohol.
3. The third part is the abbreviation for the second solvent: IPE-isopropyl ether; TEA-triethyl amine; CS<sub>2</sub> - carbon disulfide and HEX for hexane.

gradients. The permeability coefficient,  $A_G$  was calculated vs the average pressure  $\bar{P}$  across each membrane. These data were substituted into equation (8) to calculate the optimum values of  $(A_1)$ ,  $(A_2)$ ,  $R$  and  $\sigma_g$  for each membrane using each gas separately. The results are given in Tables 1-3.

The optimum value of the characterization parameters were calculated using a grid search method. In this method, the parameters  $R$  and  $\sigma_g$  were assumed which in turn determined the range of pore radius values ( $R_{min}$  and  $R_{max}$ ). The integrals  $I_1$ ,  $I_2$ ,  $I_3$ ,  $I_4$  and  $I_5$  were calculated and substituted into equation (8) which can be written as follows:

$$A_G = A_1 X_1 + A_2 X_2 \quad (15)$$

Table 2 Membrane characterization by using  $\text{CO}_2$  permeation data

Membrane	$(\bar{R})_{\text{CO}_2} \times 10^{10}$ , m	$(\sigma_g)_{\text{CO}_2} \times 10^{10}$ , m	$(A_1)_{\text{CO}_2} \times 10^{-20}$ , m <sup>-3</sup>	$(A_2)_{\text{CO}_2} \times 10^8$ , kmol/m <sup>3</sup> s Pa <sup>2</sup>
CA70-M-IPE	6.50	1.01	0.326	3.264
CA75-M-IPE	4.00	1.01	2.661	5.169
CA90-M-IPE	3.50	1.01	1.141	0.858
CA70-E-IPE	4.50	1.10	2.035	10.977
CA85-E-IPE	5.00	1.10	0.788	5.160
CA70-M-TEA	4.75	1.10	0.346	2.272
CA80-M-TEA	3.75	1.10	2.447	4.575
CA90-M-TEA	4.75	1.20	4.989	7.484
CA70-E-TEA	5.00	1.10	3.774	4.366
CA85-E-TEA	4.00	1.20	15.152	11.119
CA90-E-TEA	8.25	1.10	0.913	2.519
CA70-M-HEX	3.50	1.10	3.414	4.706
CA80-M-HEX	3.00	1.10	3.875	2.670
CA90-M-HEX	2.75	1.20	10.593	7.572
CA80-E-HEX	2.75	1.01	1.896	1.856
CA70-E-CS <sub>2</sub>	4.50	1.20	4.324	6.784
CA85-E-CS <sub>2</sub>	4.75	1.10	2.215	3.640
CA90-E-CS <sub>2</sub>	2.75	1.10	13.040	9.610

Table 3 Membrane characterization by using  $\text{CH}_4$  permeation data

Membrane	$(\bar{R})_{\text{CH}_4} \times 10^{10}$ , m	$(\sigma_g)_{\text{CH}_4} \times 10^{10}$ , m	$(A_1)_{\text{CH}_4} \times 10^{-20}$ , m <sup>-3</sup>	$(A_2)_{\text{CH}_4} \times 10^8$ , kmol/m <sup>3</sup> s Pa <sup>2</sup>
CA70-M-IPE	3.25	1.01	0.060	0.190
CA75-M-IPE	4.25	1.10	0.604	1.054
CA90-M-IPE	5.75	1.90	0.040	0.236
CA70-E-IPE	2.75	1.10	9.950	4.651
CA85-E-IPE	3.25	1.30	0.586	0.766
CA70-M-TEA	1.00	1.70	5.454	0.695
CA80-M-TEA	2.50	1.20	4.322	3.844
CA90-M-TEA	6.50	1.60	0.751	2.288
CA70-E-TEA	7.75	2.00	0.321	0.275
CA85-E-TEA	12.25	1.10	1.330	0.979
CA90-E-TEA	2.50	1.50	5.427	3.568
CA70-M-HEX	2.25	1.30	3.487	1.050
CA80-M-HEX	1.00	1.90	7.185	0.631
CA90-M-HEX	1.75	1.70	3.186	1.315
CA80-E-HEX	1.00	2.40	0.569	0.248
CA70-E-CS <sub>2</sub>	4.50	1.40	0.934	2.598
CA85-E-CS <sub>2</sub>	1.50	1.70	5.165	1.833
CA90-E-CS <sub>2</sub>	3.50	1.40	1.054	1.700

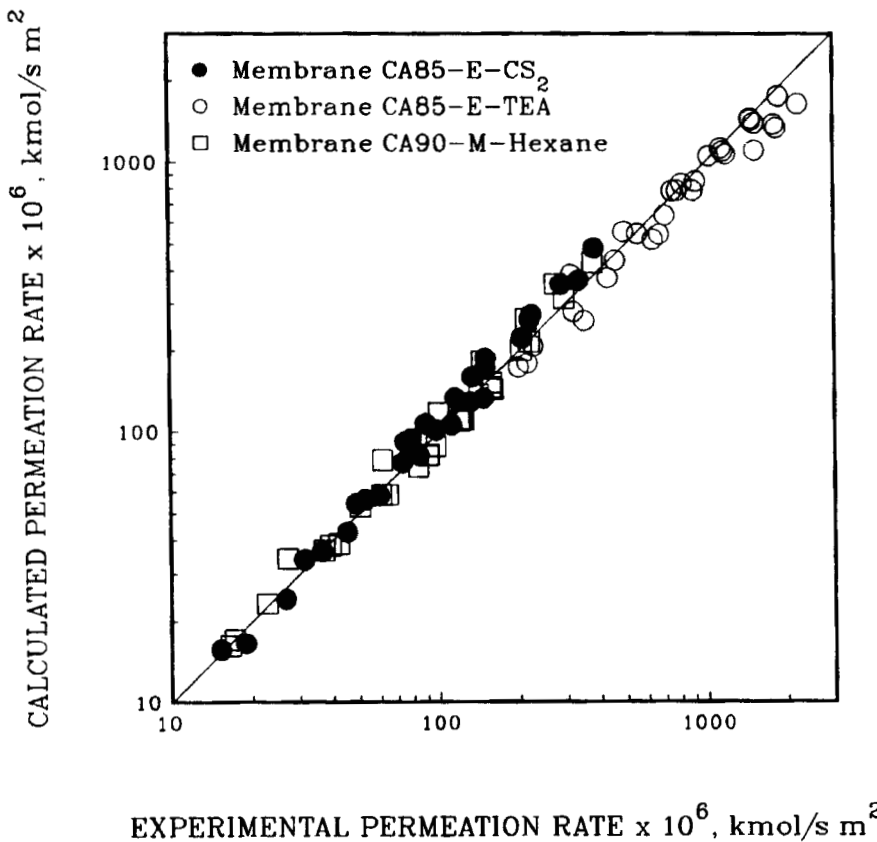


FIGURE 2 Comparisons of experimental and calculated permeation rates of  $\text{CO}_2/\text{CH}_4$  gas mixture.

where

$$X_1 = G_1 I_1 + G_2 I_2 + G_3 I_3, \text{ and } X_2 = \frac{I_4}{I_5} \bar{p} \quad (16)$$

A non-linear regression computer routine was used to evaluate the optimum values of the remaining parameters  $A_1$  and  $A_2$ . For each combination of  $\bar{p}$  and  $\sigma_g$ , the sum of squared residual was calculated according to the equation

$$SS_R = \sum_{i=1}^n (y_i - y_i^c)^2 \quad (17)$$

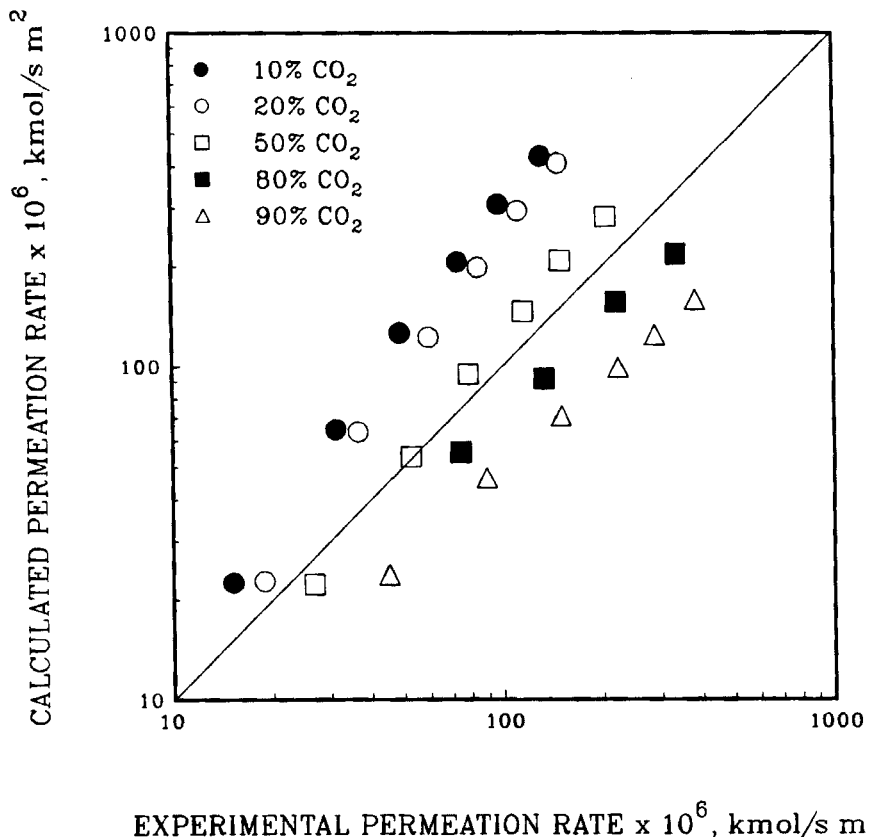


Figure 3 Effect of feed gas composition on the permeation rate prediction using approach (1) for the membrane CA90-M-HEXANE

$$\begin{aligned}
 (\bar{R})_{\text{He}} &= 1.00 \times 10^{-10} \text{ m} & (\sigma_g)_{\text{He}} &= 2.30 \times 10^{-10} \text{ m} \\
 (\bar{R})_{\text{CO}_2} &= 2.75 \times 10^{-10} \text{ m} & (\sigma_g)_{\text{CO}_2} &= 1.20 \times 10^{-10} \text{ m} \\
 (\bar{R})_{\text{CH}_4} &= 1.75 \times 10^{-10} \text{ m} & (\sigma_g)_{\text{CH}_4} &= 1.70 \times 10^{-10} \text{ m}
 \end{aligned}$$

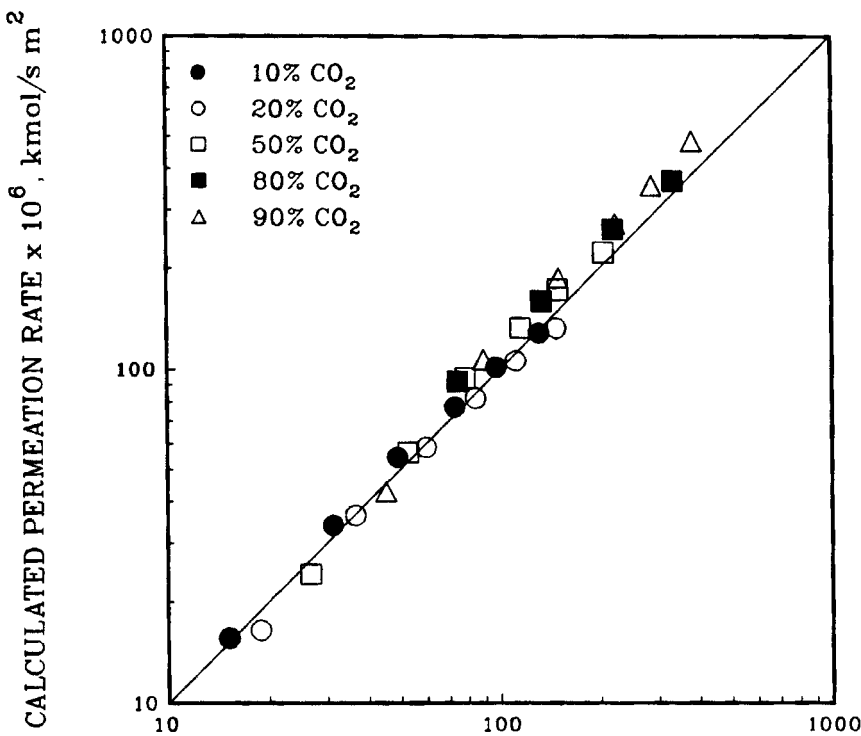


Figure 4 Effect of feed gas composition on the permeation rate prediction using approach (2) for the membrane CA90-M-HEXANE

$$\begin{aligned}
 (\bar{R})_{\text{He}} &= 1.00 \times 10^{-10} \text{ m} & (\sigma_g)_{\text{He}} &= 2.30 \times 10^{-10} \text{ m} \\
 (\bar{R})_{\text{CO}_2} &= 2.75 \times 10^{-10} \text{ m} & (\sigma_g)_{\text{CO}_2} &= 1.20 \times 10^{-10} \text{ m} \\
 (\bar{R})_{\text{CH}_4} &= 1.75 \times 10^{-10} \text{ m} & (\sigma_g)_{\text{CH}_4} &= 1.70 \times 10^{-10} \text{ m}
 \end{aligned}$$

and the procedure was repeated at all the grid points and the parameters representing the minimum value of the objective function ( $SS_R$ ) was chosen to represent the characterization parameters of the membrane under consideration.

The characterization parameters tabulated in Tables 1-3 indicate that  $A_1$  values were close for the three gases. However,  $A$  parameter although was similar for helium and  $CO_2$  gases, but was in general, much lower for  $CH_4$ . The values of  $A_2$  reflect the change in magnitude of sorption contribution to the gas total permeation. Thus, the membranes under consideration have different affinities for  $CH_4$  than for either helium or  $CO_2$ . In fact, it is possible to use the characterization parameters calculated from helium permeation data to predict the permeation rate of  $CO_2$  without expecting much error. On the other hand we should expect considerable errors if we attempted to use helium parameters to calculate the permeation rate of  $CH_4$  in the same membrane.

#### Agreement of Predicted and Experimental Permeation Rates for $CO_2/CH_4$ Mixture

The prediction of the total gas mixture permeation rate, [PR] was attempted according to the procedure followed by Mazid et al. (16) which relies on the permeation data of the reference gas and corrects for the parameters  $A_2$  and  $R_1$  according to Equations (13) and (14) respectively. There was a large scatter in the data, and the calculated permeation rates were either overpredicted or underpredicted; hence, this approach was not satisfactory to predict the permeation rates of  $CO_2/CH_4$  gas mixture.

In the second approach, the characterization parameters ( $\bar{R}$ ,  $\sigma_g$ ,  $A_1$ ,  $A_2$ ) evaluated for both components ( $CO_2$  and  $CH_4$ ) were used to predict the permeation rates using the same model equations. The permeation rates calculated from this approach are shown in Figure 2 for three different membranes. The excellent agreement between the predicted and the experimental values in Fig. 2, testifies to the success of this approach in applying the Surface Force-Pore Flow model to predict the permeation rates of binary gas mixtures. Also, it is clear that approach 1 can lead to considerable errors in predicting the permeation rates, since the contribution of the surface force can vary widely from one gas to another. However, this problem can be avoided when the characterization parameters of each of  $CH_4$  and  $CO_2$  are used (Approach 2).

#### Effect of Feed Composition

In order to investigate the correlation between the feed composition and the accuracy of predicting the permeation rate, the data shown in Figure 2 for the membrane (CA90-M-Hexane), are

plotted in Figures 3 and 4 for approaches (1) and (2) respectively. Figure 3 shows that approach (1) causes noticeable segregation between different feed compositions. On the other hand, when the calculations were done using the second approach (see Figure 4), the segregation almost disappeared and the predictions are more accurate.

### CONCLUSION

The characterization parameters of the Surface Force-Pore Flow model were evaluated using permeation data of helium,  $\text{CO}_2$  and  $\text{CH}_4$  respectively.

The permeation rates for binary  $\text{CO}_2/\text{CH}_4$  gas mixture were successfully predicted by using the characterization parameters calculated from the permeation data of single components ( $\text{CO}_2$  and  $\text{CH}_4$ ).

The pore size distribution parameters ( $\bar{R}$  and  $\sigma_g$ ) of the reference gas, can be useful only in cases where they have similar values of  $\bar{R}$  and  $\sigma_g$  for both components of the binary gas mixture. Otherwise, the predicted values for various feed compositions are not accurate. Only the characterization parameters for actual components of the binary gas mixture should be used to apply the Surface Force-Pore Flow model.

### NOMENCLATURE

- $A_1$  = constant for a given membrane related to the porous structure,  $\text{m}^{-3}$
- $A_2$  = constant related to surface transport,  $\text{kmol}/(\text{m}^3 \text{s Pa}^2)$
- $A_G$  = gas permeability coefficient,  $\text{kmol}/(\text{m}^2 \text{s Pa})$
- $c$  = mean speed of the gas molecules,  $\text{m/s}$
- $G_1, G_2, G_3$  = constants depending on the physicochemical properties of gases given by Equation 5
- $I_1, I_2, I_3, I_4, I_5$  = numerical values of integrals dependent on the porous structure
- $J_{\tilde{j}}$  = flux of gas  $\tilde{j}$ ,  $\text{kmol}/\text{m}^2 \text{s}$
- $M$  = molecular weight of the gas,  $\text{kg}/\text{kmol}$
- $N(R)$  = number of pores having a radius  $R$ ,  $\text{m}^{-1}$
- $N_t$  = total number of pores, having a radii from  $R_{\min}$  to  $R_{\max}$
- $n$  = number of data points
- $P_2$  = pressure (absolute) on the high pressure side of the membrane,  $\text{Pa}$
- $P_3$  = pressure (absolute) on the low pressure side of the membrane,  $\text{Pa}$
- $\Delta P$  = pressure differential across the membrane,  $\text{Pa}$
- $\bar{P}$  = mean pressure across the membrane,  $\text{Pa}$
- $[PR]$  = permeation rate,  $\text{kmol}/\text{s} \cdot \text{m}^2$

$Q_g$ ,  $Q_k$ ,  $Q_{s1}$ ,  $Q_v$ ,  $Q_s$ ,  $Q_T$  = quantity of gas transported in the gas phase, by Knudsen, slip, viscous, and surface flow mechanisms and total quantity of gas transported, respectively, kmol/s

$q_k$ ,  $q_v$ ,  $q_{s1}$  = quantity of gas transported through a single capillary by Knudsen, viscous, and slip flow mechanisms, respectively, kmol/s

$R$  = pore radius, m

$R_g$  = gas constant

$R_m$  = mean pore radius, m

$R_{max}$  = pore radius of the largest pore, m

$R_{min}$  = pore radius of the smallest pore, m

$S$  = membrane area,  $\text{m}^2$

$SS_R$  = sum of squared residuals defined by Equation 17

$T$  = absolute temperature, K

$x_{\tilde{i}2}$  = mole fraction of gas  $\tilde{i}$  on the high pressure side

$x_{\tilde{i}3}$  = mole fraction of gas  $\tilde{i}$  on the permeate side

$x_1$ ,  $x_2$  = variable defined by Equation 15

$y_i$  = experimental value of gas permeability coefficient,  $\text{kmol}/\text{m}^2 \text{ s Pa}$

$y'_i$  = predicted value of gas permeability coefficient,  $\text{kmol}/\text{m}^2 \text{ s Pa}$

### Greek Letters

$\Delta_{\tilde{i}}$  = radius correction factor, a constant for gas  $i$  for a given membrane material, m

$\delta$  = equivalent thickness of the membrane, m

$\eta$  = coefficient of viscosity of gases,  $\text{Pa} \cdot \text{s}$

$\lambda$  = mean free path of gases, m

$\sigma_g$  = geometric standard deviation for the log-normal pore size distribution

$\phi_{\tilde{i}}$  = relative surface transport coefficient ( $= (A_2)_{\tilde{i}} / (A_2)_{ref}$ ), related to gas-membrane interaction and defined by Equation 13

### Subscripts

$\tilde{1}$  = carbon dioxide

$\tilde{2}$  = methane

### REFERENCES

- (1) W. MacDonald and C. Pan, "Method of Drying Water-Wet Membranes", U.S. Patent 3,842,515, October 22 (1974).
- (2) P. Manos, "Membrane Drying Process", U.S. Patent 4,080,743, March 28 (1978).

- (3) P. Manos, "Gas Separation Membrane Drying with Water Replacement Liquid", U.S. Patent 4,080,744, March 28 (1978).
- (4) P. Manos, "Solvent Drying of Cellulose Ester Membranes", U.S. Patent 4,068,387, Jan. 17 (1978).
- (5) P. Manos, "Solvent Exchange Drying of Membranes for Gas Separation", U.S. Patent 4,120,098 (1978).
- (6) B.S. Minhas, T. Matsuura and S. Sourirajan, "Solvent-Exchange Drying of Cellulose Acetate Membranes for Separation of Hydrogen-Methane Gas Mixtures", ACS Symposium Series, S. Sourirajan and T. Matsuura, Eds., vol. 281, paper 33, pp. 451-466 (1984).
- (7) R. Rangarajan, M.A. Mazid, T. Matsuura and S. Sourirajan, "Permeation of Pure Gases Under Pressure Through Asymmetric Porous Membranes. Membrane Characterization and Prediction of Performance", Ind. Eng. Chem. Process Des. Dev. 23, pp. 79-87 (1984).
- (8) S. Sourirajan and T. Matsuura, "Reverse Osmosis/Ultrafiltration Process Principle", National Research Council of Canada, Ottawa, 1985, p. 5.
- (9) P. Mears, "Fundamental Mechanisms of Transport of Small Molecules in Solid Polymers", Proceedings of the Fourth BOC Priestley Conference, Leeds, Sept. 16 - 18, 1986, pp. 1 - 25.
- (10) W.R. Vieth, J.M. Howell and J.H. Hsieh, J. Membrane Sci., 1, 177, 1976
- (11) T. Matsuura and S. Sourirajan, "Reverse Osmosis Transport Through Capillary Pores Under the Influence Surface Force", Ind. Eng. Chem. Process Des. Dev., 20, 273 (1981).
- (12) H.W. Liepmann, J. Fluids Mechanics, 10, 65 (1961).
- (13) D.E. Stahl, "Transition Range Flow Through Microporous Vycor", Ph.D. Thesis, Chem. Eng. Dept., The University of Iowa, Iowa City, IA (1971).
- (14) R.D. Present, "Kinetic Theory of Gases", McGraw-Hill, New York, P.61 (1958).
- (15) C.R. Metz, "Physical Chemistry", McGraw-Hill, New York, 1976; p.11.
- (16) M.A. Mazid, Rangarajan, T. Matsuura, S. Sourirajan, "Separation of Hydrogen-Methane Gas Mixture by Permeation Under Pressure Through Porous Cellulose Acetate Membranes", Ind. Eng. Chem. Process Des. Dev., 24, 907 (1985).